

The Heavy Ion Physics Program with ATLAS at the LHC

N. Grau¹ *for the ATLAS Collaboration*

¹ Columbia University, Nevis Labs,
Irvington, NY, 10533, USA

Abstract. The first Pb+Pb collisions at the Large Hadron Collider (LHC) at $\sqrt{s_{NN}} = 5.52$ TeV are imminent. Heavy ion collisions at the LHC provide an extended energy lever arm to the existing measurements made at RHIC and SPS, especially in hard (large- Q^2) processes. In this contribution an overview of the ATLAS detector is given and the current physics focus of Heavy Ion Working Group is discussed.

Keywords: heavy-ion, multiplicity, jets, quarkonia, ATLAS, LHC

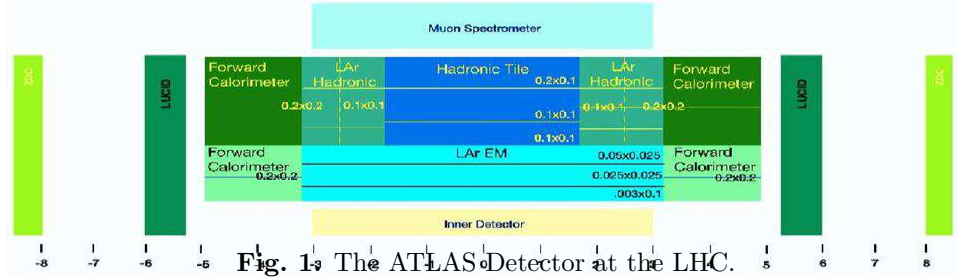
PACS: 25.75.-q

1. Introduction

The Large Hadron Collider is expected to collide $p + p$ and $Pb + Pb$ collisions in the very near future at the new energy frontier for both nuclear and high energy physics. With the many exciting results from the hard scattering, high- Q^2 , processes at RHIC such as high- p_T particle suppression or jet quenching[1] and heavy flavor production[2], the heavy ion physics program at the LHC is compelling. The rate for jets and heavy flavors are substantial compared to RHIC[3]. This contribution outlines the heavy ion program of the ATLAS detector[4]. First, a description of the ATLAS detector is detailed. Then a description of the physics program is outlined with specific examples of measurements of global variables, jet reconstruction, heavy flavor physics and low-x physics.

2. The ATLAS Detector

The ATLAS detector[5] (Fig. 1) is a large, multi-purpose detector designed for detecting and reconstructing high- p_T observables in $p + p$ collisions. It is composed of an inner tracking system, electromagnetic and hadron calorimeters, and a muon spectrometer. Even though ATLAS was designed for $p + p$ multiplicities, occupancies for central Pb+Pb HIJING events are low enough for most subsystems for use as a



heavy ion detector.

The inner tracking system covers full azimuth and approximately $|\eta| < 2.5$ and is within a 2T solenoidal field. It consists of three pixel layers ($r=50.5$ mm, 88.5 mm and 122.5 mm), followed outward by four layers of double-sided silicon strip detectors, and finally the transition radiation tracker a straw tracker with 35 points for $|\eta| < 2.5$ and $p_T > 0.5$ GeV. With initial studies using central HIJING events the occupancy of the pixel layers are less than 2% and the silicon strips are less than 20%. However, the occupancy for the transition radiation tracker is large. As such, heavy ion tracking is being optimized with the 11 space points from the pixels and the strips.

The calorimeter coverage in ATLAS is full azimuth and $|\eta| < 5$ with several radial (longitudinal) segments. The barrel region ($|\eta| < 1.5$) consists of a thin presampler to measure lost energy in material before the calorimeter, three longitudinal segments of liquid argon (LAr) electromagnetic calorimeters, and followed by three longitudinal segments of tile hadronic calorimeters. The endcap region ($3.2 < |\eta| < 1.5$ units) is composed of the same LAr electromagnetic calorimetry as the barrel. The hadronic calorimeter consists of two longitudinal segments of copper plates. Finally the the forward ($4.9 < |\eta| < 3.2$ units) hadronic calorimeter has three segments.

The $\eta - \phi$ segmentation of the calorimeters is dependent on the longitudinal segment. The front (strip) layer of the barrel LAr calorimeter is composed of cells with a typical $\Delta\eta \times \Delta\phi$ of 0.003×0.1 . Such fine granularity was built into the calorimeter for vectoring $H \rightarrow \gamma\gamma$ events. The middle layer of the LAr calorimeter has a typical segmentation of 0.025×0.025 and has the largest interaction length of the barrel. Most electromagnetic energy is deposited within the middle layer. The back layer of the LAr calorimeter has a typical segmentation of 0.05×0.025 . The barrel tile calorimeter has a typical segmentation of 0.1×0.1 , 0.1×0.1 , and 0.2×0.2 in $\Delta\eta \times \Delta\phi$ in the front, middle, and back layer. In what is shown later,

towers of 0.1×0.1 are composed from the sum of cells from all layers and used in jet reconstruction and elliptic flow (v_2) analyses.

Beyond the hadronic calorimeters and within a toroidal field is the muon spectrometer, one of the largest ever constructed, with acceptance of muons out to $|\eta| < 2.7$ units. It consists of three chambers containing drift tubes (in the midrapidity, barrel region) or cathode strip chambers (in the forward rapidities) to measure the R-z position of the tracks passing through the chambers. The occupancy is very low since the hadronic calorimeters absorb nearly all of the hadronic background.

The Zero Degree Calorimeter (ZDC) is located at $\eta = \pm 8$ and will consist of 2 hadronic calorimeter modules with a shower maximum detector. These will be preceded by a highly segmented electromagnetic calorimeter module. The ZDC is designed for triggering and centrality definition as well as forward meson measurements.

3. The Heavy Ion Physics Program^a

With the ATLAS detector it is possible to cover a broad range of physics observables. Currently the Heavy Ion Working Group has been focused on global physics measurements such as $dN_{ch}/d\eta$ and v_2 , jet measurements from the longitudinally segmented calorimeter, charm and bottom quarkonia measurements using the muon spectrometer, and low-x physics observables utilizing the ZDC [6].

A crucial first measurement during heavy ion collisions at LHC is the particle multiplicity density, $dN_{ch}/d\eta$. Currently, for example, extrapolation of a logarithm-

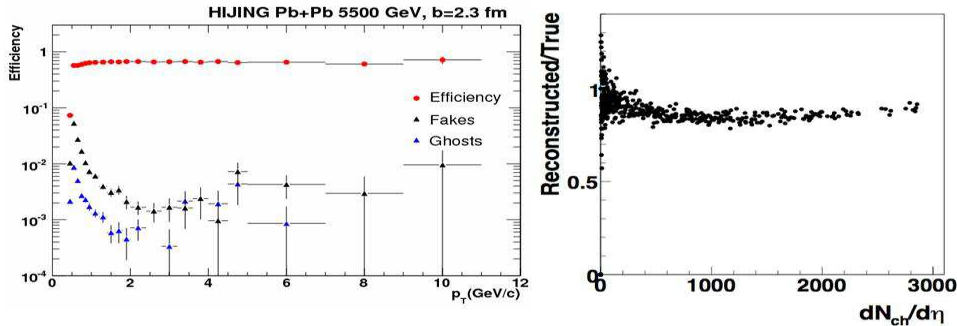


Fig. 2. *Left:* Efficiency, ghost rate, and fake rates (see text) as a function of track p_T for tracking optimized for heavy ion events. *Right:* Comparison of reconstruction $dN_{ch}/d\eta$ from tracklets (see text) compared to the HIJING generated $dN_{ch}/d\eta$ as a function of generated $dN_{ch}/d\eta$.

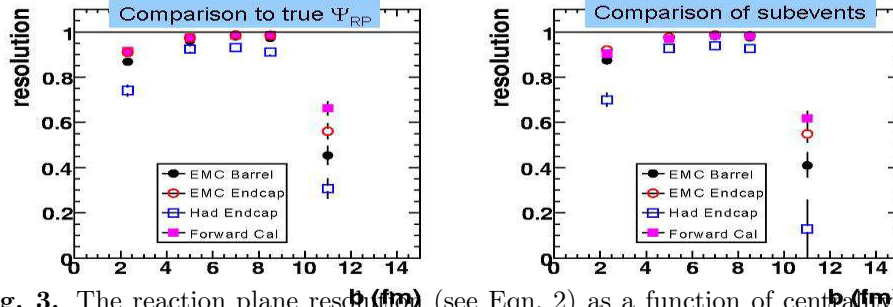


Fig. 3. The reaction plane resolution (see Eqn. 2) as a function of centrality by comparing fitted Ψ_{RP} and the generated Ψ_{RP} (left) and comparing Ψ_{RP} 's fitted from positive and negative η regions (right).

mic dependence of the $dN/d\eta/\langle 0.5N_{part} \rangle$ based on measured data at lower energies is 50% lower than the Color Glass Condensate (CGC) prediction [7]. HIJING multiplicities with and without quenching are even larger.

Using the pixels and strips of the inner detector, it is expected that, with good efficiency, tracking will extend below 1.0 GeV/c. The left panel of Fig. 2 shows the efficiency and fraction of ghost^b and fake^c tracks as a function of track p_T . The 1.0 GeV/c cut off is artificial and considerable effort is being made to extend the tracking to as low p_T as possible. Early attempts indicate that tracking down to 400 MeV/c will be possible. Such particles pass through all layers of tracking and reach the calorimeter with a shallow entrance angle.

An alternative approach to measure $dN_{ch}/d\eta$ including low- p_T particles is to perform tracklet reconstruction [8] by pairing hits in the first two pixel layers. The right panel of Fig. 2 shows the ratio of measured to generated $dN_{ch}/d\eta$ as a function of generated $dN_{ch}/d\eta$. A very good reproduction of $dN_{ch}/d\eta$ is seen for all values of $dN_{ch}/d\eta$.

Another global observable of great interest at LHC energies is v_2 . At midrapidity, the single particle distribution can be written as

$$\frac{dN}{d\phi dp_T} = \frac{N}{2\pi} (1 + 2v_2 \cos(2(\phi - \Psi_{RP}))) \quad (1)$$

where Ψ_{RP} is the reaction plane angle. At RHIC, large values and scaling properties of v_2 for all measured particles indicate that a strongly-coupled, low-viscosity partonic stage exists at RHIC [9]. The non-viscous, hydrodynamical properties of the matter created at RHIC is apparently due to the fact that the v_2/ϵ is at the hydrodynamic limit. At higher energies, a saturation of this value is expected. However, other effects, such as path-length dependent energy loss, could drive the

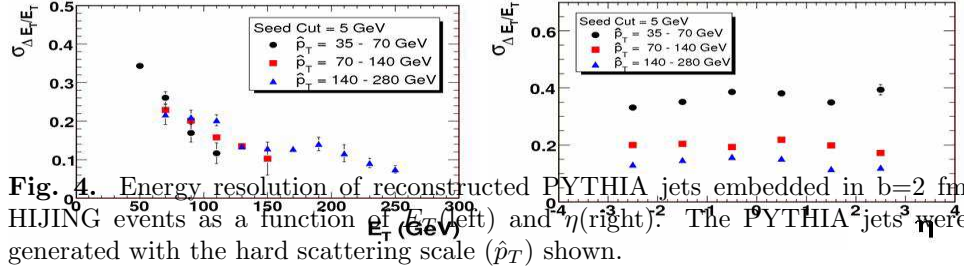


Fig. 4. Energy resolution of reconstructed PYTHIA jets embedded in $b=2$ fm HIJING events as a function of E_T (left) and η (right). The PYTHIA jets were generated with the hard scattering scale (\hat{p}_T) shown.

observed v_2 to larger values at LHC energies. This increasing trend of v_2/ϵ is seen in the data from SPS to RHIC energies [11].

It is possible, using the ATLAS calorimeter, to determine Ψ_{RP} and v_2 values event-by-event. A realistic flow was simulated based on the observed RHIC data for $v_2(p_T, \eta, \text{cent})$. HIJING events were run through an afterburner where all particles' azimuthal angles are altered based on the prescription outlined in ref. [12]. Calorimeter E_T distributions are then fit with Eqn. 1 to obtain the value of v_2 and Ψ_{RP} . To evaluate the goodness of the reaction plane determination, the resolution of the reaction plane, defined as

$$\text{res} = \langle \cos [2 (\Psi_{\text{RP,fit}} - \Psi_{\text{RP,gen}})] \rangle \quad (2)$$

is evaluated. This is shown in Fig. 3 for different calorimeter regions and as a function of centrality. The right plot of Fig. 3 shows the resolution based on comparison of subevents from positive and negative η . Both resolutions are near unity. The resolution as evaluated by the subevent technique is consistent with the direct comparison to the generated Ψ_{RP} , giving confidence that the subevent measurement of the reaction plane is accurate.

A key strength of the ATLAS detector is the calorimetry. At LHC jets of large energy ($E_T > 40$ GeV) will be produced quite copiously[3]. With a hermetic calorimeter event-by-event jet reconstruction is possible even within the heavy ion underlying event. Such event-by-event information should yield greater insights into partonic energy loss discovered at RHIC. For complete details of the jet reconstruction and capabilities of the ATLAS detector see ref. [10].

Jets are studied by embedding PYTHIA jets directly into HIJING simulated events. Background subtraction schemes have been developed to remove the large underlying event from the HIJING. A standard jet reconstruction technique is the cone algorithm which sums energy within a given radius, $R = \sqrt{\Delta\phi^2 + \Delta\eta^2}$ of a reconstructed jet axis. Typically these algorithms are seeded by calorimeter towers. Fig. 4 shows the energy resolution as a function of jet E_T and jet η from a $R=0.4$

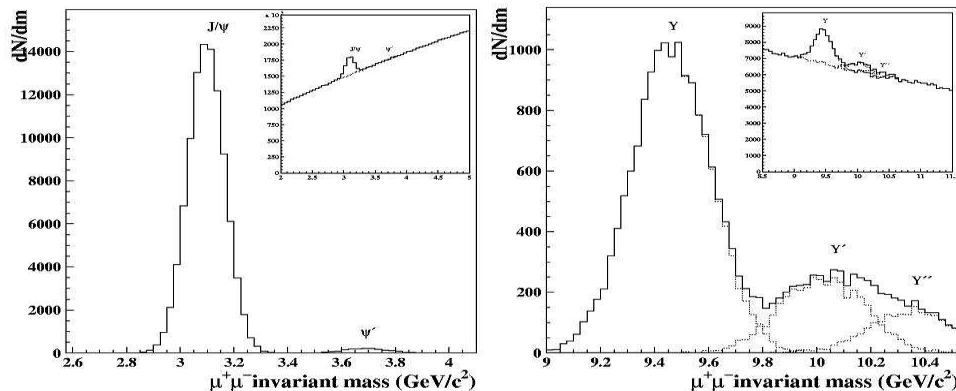


Fig. 5. Di-muon invariant mass distribution for charm quarkonia (left) and bottom quarkonia (right) expected from the ATLAS muon spectrometer. The right plot is for ψ 's with decay muons $|\eta| < 2$.

cone algorithm with a seed tower of 5 GeV.

There are also two important features of the ATLAS calorimeter. First, for the background subtraction, nearly 60% of the underlying event ranges out in the strip layer of the calorimeter. This is due to the large bending of $p_T < 1$ GeV/c charge particles in the magnetic field. The bend is large enough that the particles enter the calorimeter at a steep angle and deposit all of their energy at the front of the calorimeter. This significantly reduces the background in the other longitudinal calorimeter layers.

The other important feature of the ATLAS calorimeter is the strip layer of the barrel electromagnetic calorimeter. The strip layer makes it possible to detect and reject $\pi^0 \rightarrow \gamma\gamma$ decays from direct photon events. Studies in p+p collisions with pile up indicate that a rejection factor of 4 can be gained by information in the strip layer without a jet isolation cut [13]. Initial studies from HIJING events indicate that even in central events the occupancy in the strip layers is so low that the background is negligible for even fairly low photons. It is possible, then, that a rejection > 1 can be reached in heavy ion events prior to an isolation cut. Such rejection is important since the background itself will be directly measurable. This is an area that considerable effort is currently being directed.

Heavy quarkonia and its suppression and regeneration is still an unresolved topic. Currently RHIC results show a J/Ψ suppression similar to that measured at SPS [14]. Recent lattice calculations indicate that different quarkonia states disassociate at different temperatures [15]. This suggest that a measurement of

quarkonia suppression of the different states yields the temperature of the matter produced.

The ATLAS muon spectrometer is utilized to measure and study heavy quarkonia by their $\mu^+\mu^-$ decays. Both charm and bottom will be accessible in ATLAS. The Di-muon invariant mass distributions are shown in Fig. 5. The resolution is sufficient to distinguish the J/Ψ and the Ψ' as well as the Υ from the higher Υ states. Studies of the Υ mass resolution and acceptance indicate the resolution is $120 \text{ MeV}/c^2$ at midrapidity, increasing at higher η . The acceptance extends to ± 6 units of pseudorapidity for Υ down to $p_T = 0 \text{ GeV}/c$ [16].

Another avenue that is currently being explored is the photon capability to measure the $\chi_c \rightarrow J/\Psi + \gamma$. This would allow a direct measurement of the feeddown to the J/Ψ and yield an important state on the thermometer of the quark-gluon plasma.

A unique feature of the ATLAS ZDC is the high-resolution electromagnetic module. The resolution is designed to detect photons from very forward meson decays. An example of the expected di-photon invariant mass distribution is given in the left panel of Fig. 6. The location of the ZDC at and beyond η of ± 8 units provides unprecedented low- x coverage for A+A collisions. A plot of the p_T and x range accessible by the ZDC is shown in the right panel of Fig. 6. At modest p_T values of x of the order of $10^{-6} - 10^{-7}$ can be reached. This region may well be within the saturation regime making possible study of the effects of the Color Glass Condensate.

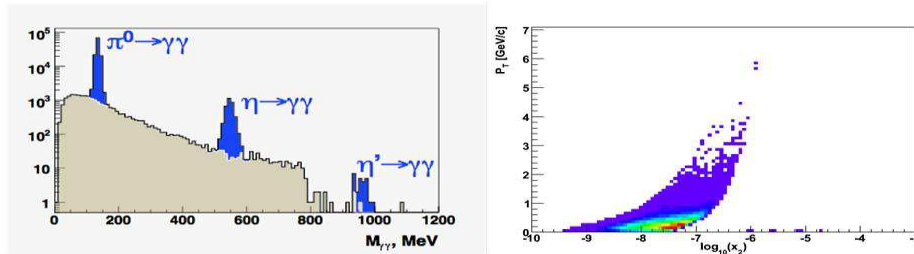


Fig. 6. *Left:* Di-photon invariant mass distribution for forward produced mesons reconstructed by the ZDC. *Right:* Coverage in p_T - x space of forward mesons seen by the ZDC.

4. Summary

The ATLAS detector was designed for p+p collision studies but is well suited for studying $A + A$ collisions at the LHC. Utilizing the unique aspects of the ATLAS detector, e.g. the calorimeter segmentation for prompt photon measurements or the ZDC resolution for low-x physics, a broad set of physics topics will be covered with the ATLAS detector. This contribution has outlined a small subset of the possible measurements with ATLAS. These measurements may help in understanding features of RHIC data and/or they may also uncover new and yet unforeseen scenarios at the next energy frontier.

Notes

- a.* The figures shown here were based on studies using modified versions of ATLAS production software. Thus, they should be considered ATLAS preliminary. For completeness, we list the version of Athena software used for each figure: Fig. 2(right) used 12.0.31 with a new tracking algorithm while Fig. 2(left) and Figure 3 used 12.0.3. Fig. 4 used 11.0.41 and special background subtraction algorithms.
- b.* **Ghost** - A track which, along with multiple other tracks, matches a generated track
- c.* **Fake** - A track with no matching generated track

References

1. S. S. Adler *et al.* (PHENIX Collaboration), nucl-ex/0611007
2. A. Adare *et al.* (PHENIX Collaboration), *Phys. Rev. Lett.* **98**, 172301 (2007)
3. A. Accardi, N. Armesto, and I. P. Lokhtin, Contribution to the Yellow report on Hard Probes in Heavy Ion Collisions at the LHC, hep-ph/0211314
4. ATLAS Heavy Ion Physics Letter of Intent, CERN-LHCC-2004-009
5. ATLAS Technical Design Report Volume 1, CERN-LHCC-99-14
ATLAS Technical Design Report Volume 2, CERN-LHCC-99-15
6. P. Steinberg (for the ATLAS Collaboration), arXiv:0705.0382 [nucl-ex].
7. D. Kharzeev, E. Levin, and M. Nardi *Phys. Rev.* **C71** (2005) 054903.
8. B. B. Back *et al.* (PHOBOS Collaboration), *Phys. Rev. Lett.* **85**, 3100 (2000)
9. A. Adare *et al.* (PHENIX Collaboration), nucl-ex/0608033
10. W. Holzmann, these proceedings
11. C. Alt *et al.*, *Phys. Rev.* **C68**, 034903 (2003)
12. A. M. Poskanzer and S. A. Voloshin, *Phys. Rev.* **C58** 1671 (1998)
13. P. Schwemling, (for the ATLAS Collaboration), *Eur. Phys. J.* **C34** s129 (2004)
14. A. Adare *et al.*, (PHENIX Collaboration), nucl-ex/0611020.
15. M. Asakawa and T. Hatsuda, *Phys. Rev. Lett.* **92**, 012001 (2004)

16. L. Rosselet, (for the ATLAS Collaboration) *Springer Proceedings in Physics*
108, 206 (2006)